International Journal of Applied Mechanics
Vol. 1, No. 3 (2009) 405–420


ICP Imperial College Press
www.icpress.co.uk

# A MULTI-SCALE NONEQUILIBRIUM MOLECULAR DYNAMICS ALGORITHM AND ITS APPLICATIONS

NI SHENG

*Department of General Studies*
*Macau University of Science and Technology, Macau, China*

SHAOFAN LI*

*Department of Civil and Environmental Engineering*
*University of California, Berkeley, CA 94720, USA*
*shaofan@berkeley.edu*

Received 11 May 2009
Accepted 17 May 2009

In this paper, we introduce a *multi-scale nonequilibrium molecular dynamics* (MS-NEMD) model that is capable of simulating nano-scale thermal–mechanical interactions. Recent simulation results using the MS-NEMD model are presented. The MS-NEMD simulation generalises the nonequilibrium molecular dynamics (NEMD) simulation to the setting of concurrent multi-scale simulation. This multi-scale framework is based on a novel concept of *multi-scale canonical ensemble*. Under this concept, each coarse scale finite element (FE) node acts as a thermostat, while the atoms associated with each node are assumed to be in a local equilibrium state within one coarse scale time step. The coarse scale mean field is solved by the FE method based on a coarse-grained thermodynamics model; whereas in the fine scale the NEMD simulation is driven by the random force that is regulated by the inhomogeneous continuum filed through a *distributed Nośe–Hoover thermostat network*. It is shown that the fine scale distribution function is canonical in the sense that it obeys a drifted local Boltzmann distribution.

*Keywords*: Nonequilibrium thermodynamics; multi-scale simulation; canonical ensemble.



## 1. Introduction

The essence of heat transfer at small scales is the nonequilibrium thermal–mechanical multi-scale coupling, in which the length and/or time scales span from molecular level to continuum level. The fundamental understanding of nonequilibrium thermal–mechanical coupling process at small scales and the capacity to simulate such physical phenomena are vital to the study of the mechanism of energy conversion and to the advancement of reliability of micro and nano-electronics.

*Corresponding author.

The conventional molecular dynamics (MD) simulation is a simulation of micro-canonical ensemble, and it is unable to describe system's responses due to thermal fluctuation. The finite temperature equilibrium MD simulation is a simulation of canonical ensemble under fixed temperature, which is regularised by various thermostats, e.g. Nośe–Hoover thermostat [Hoover, 1985; Nośe, 1984, 1986]. However, the equilibrium MD simulation is unable to simulate problems with spatial or temporal temperature gradients. An illustration of one-dimensional Nośe–Hoover equilibrium MD simulation is given in Fig. 1(a). The thermostated region is denoted by blue colour.

Since 1970s, the nonequilibrium molecular dynamics (NEMD) method has been a major numerical tool for the simulations of nonequilibrium thermal–mechanical coupling processes, which is largely due to the contribution made by Hoover [1983] and Evans and Morriss' [1990] pioneer works. Currently, there are several types of NEMD simulations that have been used in different research fields [Baranyai, 1996; Bright and Evans, 2005; Edwards and Dressler, 2001; Evans *et al.*, 1983; Evans and Morriss, 1984, 1990; Galea and Attard, 2002; Hoover, 1980, 1983; Lepri *et al.*, 2003; Müller-Plathe, 1997; Tuckerman *et al.*, 1997; Zhang *et al.*, 2000]. Among them, the direct NEMD simulation [Baranyai, 1996; Lepri *et al.*, 2003; Müller-Plathe, 1997] is the most popular one used in practice. It has been the workhorse in performing direct atomistic or molecular simulations in many scientific and engineering fields. In the direct NEMD simulation, the system is driven out of equilibrium by prescribed boundary heat flux or temperature distribution, i.e. prescribed heat sources or heat sinks at the boundaries of the domain of interest. Such heat sources or sinks are maintained by either thermostat techniques or velocity scaling techniques. An illustration of one-dimensional direct NEMD simulation is given in Fig. 1(b).

A main shortcoming of the direct NEMD simulation is that in the interior domain it simply uses the conventional micro-canonical ensemble MD simulation, so the system cannot automatically return to a canonical ensemble equilibrium state when the boundary heat flux disappears. This fact can be illustrated in Fig. 1, in

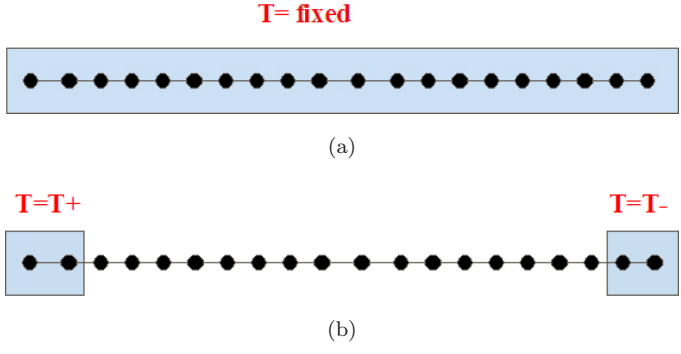


Fig. 1. Comparison between (a) the Nośe–Hoover equilibrium MD simulation and (b) the direct NEMD simulation.

which we compare the direct NEMD simulation with the Nośe–Hoover equilibrium MD simulation.

We question on whether the deterministic micro-canonical MD simulation can faithfully model the statistical phonon scattering process in the interior domain without ubiquitous presence of random forces. In a recent monograph, Chen [2005] expressed the same concern on the direct NEMD simulation. The present authors note that it may be necessary to develop a NEMD simulation technique with solid statistical mechanics foundation for direct simulations of nonequilibrium systems.

Recently, a class of concurrent multi-scale simulations have emerged in nano-scale computational mechanics, for example, the quasi-continuum method [Knap and Ortiz, 2001; Tadmor *et al.*, 1996], the coarse-grained MD method [Rudd and Broughton, 1998, 2005], the bridging scale method [Wagner and Liu, 2003; Wagner *et al.*, 2004], the finite temperature quasi-continuum method [Tang *et al.*, 2006], the perfectly matched multi-scale dynamics method [Li *et al.*, 2006; To and Li, 2005] and among others. The essence of the multi-scale simulations is the coupling of deterministic coarse scale computations with stochastic, or statistical, fine scale computations. They are suited to model Physical phenomena operating across different scales and have become a popular research topic. However, most of the multi-scale models in the literature focus either on solving problems at zero temperature or on simulating equilibrium systems with uniform environmental temperature. To the authors' best knowledge, there are few multi-scale simulations or formulations available for nonequilibrium systems.

In this paper, we report a *multi-scale nonequilibrium molecular dynamics* (MS-NEMD) model that generalises the NEMD simulation to the setting of concurrent multi-scale simulation and is capable of simulating nonequilibrium thermal–mechanical coupling processes at the atomistic scale. In the proposed MS-NEMD model, the coarse scale mean field is concurrently solved by finite element (FE) method based on a coarse-grained thermodynamics model; whereas in the fine scale the NEMD simulation is carried out.

A main difference between the proposed MS-NEMD simulation and other NEMD simulations is that in the proposed MS-NEMD simulation, the fine scale model alone cannot provide statistics details. The fine scale statistical model, by which the fine scale stochastic motions are described, depends on the coarse scale mean field in the following two ways: (i) The fine scale motion is driven out of the equilibrium by the coarse scale mean field instead of a prescribed or fictitious external field as in some traditional NEMD simulations. The amplitude of fine scale fluctuations is controlled by the coarse scale thermodynamic temperature, which is determined by coarse scale boundary heat fluxes, interior heat sources/sinks, and interior coarse scale heat diffusion and convection. (ii) In turn, the fine scale motion provides thermal fluctuation to the mean field. The fine scale simulation results are used to update temperature and displacement fields at the coarse-grained level, and they may also be used to calculate transport coefficients for the coarse-grained formulation.

It is shown that the fine scale distribution function is canonical in the sense that it obeys a drifted local Boltzmann distribution. To the authors' best knowledge, the proposed MS-NEMD algorithm is the first canonical NEMD algorithm in the literature. Moreover, when external forces and fluxes disappear, the MS-NEMD simulation will degenerate to the equilibrium MD simulation, i.e. the simulated system can automatically and spontaneously return to an equilibrium state.

This paper is organised in the following way. In Sec. 2 we outline the basic ideas of MS-NEMD model. In Secs. 3 and 4 we introduce in detail the fine scale model and the coarse scale model, respectively. One- and two-dimensional numerical examples are presented in Sec. 5. Finally, we conclude the presentation in Sec. 6 by making a few remarks.



## 2. The Basic Framework and Ideas

The foundation of the concurrent MS-NEMD simulation is the multi-scale decomposition proposed by Rudd and Broughton [1998] and Wagner and Liu [2003], which decomposes the discrete atomistic displacement field, $\mathbf{q}$, into a coarse scale part and a fine scale part:

$$\mathbf{q} = \bar{\mathbf{q}} + \mathbf{q}'. \tag{2.1}$$

The symbol $\bar{}$ indicates coarse scale quantities and the symbol $'$ indicates their fine scale counterparts.

The main ingredients of the proposed MS-NEMD are its multi-scale computation and coupling. The coarse scale motion is solved by using the FE method based on a coarse-grained thermodynamics model; whereas the fine scale motion is modelled and solved by using an NEMD. A conceptual illustration of the multi-scale framework is shown in Fig. 2. In the proposed MS-NEMD model, we argue that each coarse scale FE node may be viewed as a thermal reservoir, and it represents the ambient space of a large set of atoms. We call each set of atoms surrounding an FE node as a Voronoi cell-ensemble. Note that the Voronoi cell or Voronoi tessellation is a dual structure of Delaunay triangulation [Qiang *et al.*, 1999], hence the cell structure is related to FE mesh or discretisation (see Fig. 2).

The main novelty of this work is the proposal of the concept — *multi-scale canonical ensemble*, which is a generalisation of the classical notion of canonical ensemble. The classical canonical ensemble denotes a system embedded into an infinitely large thermal reservoir, whose temperature remains constant during an equilibrium process. In the proposed MS-NEMD model, we argue that the temperature of each coarse scale nodal reservoir remains constant during any time interval that is smaller than the time scale of the coarse grain, which is chosen here as the coarse scale time step. Since a Voronoi cell-ensemble is embedded within a coarse scale nodal reservoir, the motions of atoms in a Voronoi cell-ensemble can be assumed to reach to a local equilibrium state within one coarse scale time step. So we may call a Voronoi cell-ensemble as a *multi-scale canonical ensemble* in the sense of

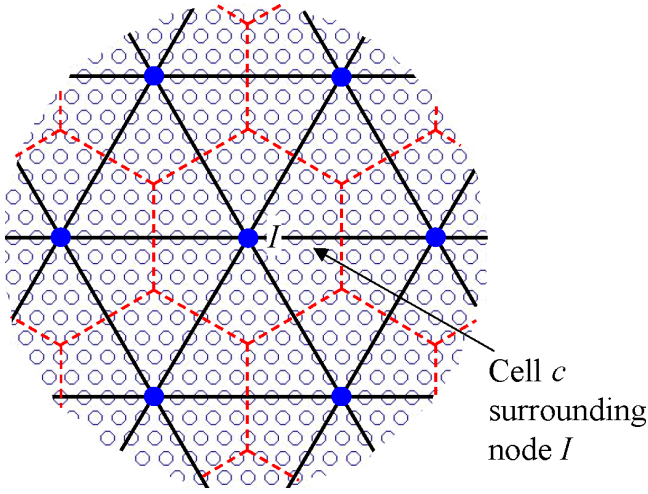


Fig. 2. Coarse-grained finite element mesh and Voronoi cell-ensemble structure.



local equilibrium approximation. The local equilibrium assumption has been widely used in nonequilibrium thermodynamics, e.g. Evans and Morriss [1990]. This work may be the first attempt to use it in multi-scale analysis.

To ensure each Voronoi cell-ensemble reaching to a local equilibrium state in each coarse scale time step, we introduce a local Nośe–Hoover thermostat in each cell-ensemble. The local thermodynamic temperature for each cell-ensemble is set as the coarse scale temperature at the governing FE node. Since the coarse scale temperature distribution is nonuniform and evolving with time, the FE nodal temperature changes from node to node and time to time. Therefore, the local thermodynamic temperature is not uniform among different cell-ensembles and different coarse scale time steps. This leads to the use of a *distributed Nośe–Hoover thermostat network* in the present MS-NEMD simulation (see Fig. 3), which is a generalisation of the Nośe–Hoover thermostat [Hoover, 1985; Nośe, 1984, 1986] in a global equilibrium ensemble MD simulation.

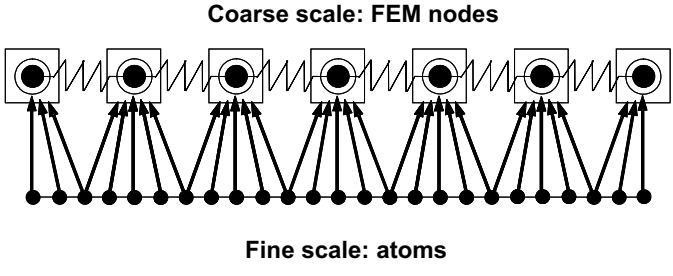


Fig. 3. The structure of distributed Nośe–Hoover thermostat network.

In statistical physics, the fluctuation dissipation theorem states that the response of a system in thermodynamic equilibrium to a small external perturbation is the same as its response to a spontaneous fluctuation. In the proposed MS-NEMD model, coarse scale thermodynamic temperature provides the external disturbance through the distributed Nośe–Hoover thermostat network, which drives the system out of equilibrium, and it is equivalent to fluctuations created by random forces. Therefore, one may view the distributed Nośe–Hoover thermostat network as a means to control the amplitude of fine scale fluctuations. This is another novelty of the present work.



## 3. The Fine Scale NEMD Model

The multi-scale displacement decomposition in Eq. (2.1) implies similar decompositions for velocity field, $\dot{\mathbf{q}}$, and linear momentum field, $\mathbf{p}$, i.e.

$$\dot{\mathbf{q}} = \dot{\bar{\mathbf{q}}} + \dot{\mathbf{q}}' \quad \text{and} \quad \mathbf{p} = \bar{\mathbf{p}} + \mathbf{p}'. \tag{3.1}$$

With the bridging scale formulation [Wagner and Liu, 2003], the total scale kinetic energy can be decoupled in terms of $\bar{\mathbf{p}}$ and $\mathbf{p}'$. This suggests the following multi-scale adiabatic Hamiltonian for a single cell-ensemble $c$ surrounding the FE node $I$

$$H_c^{\text{adia}} = \sum_{i=1}^{n_c} \frac{1}{2m_i} \bar{\mathbf{p}}_i \cdot \bar{\mathbf{p}}_i + \sum_{i=1}^{n_c} \frac{1}{2m_i} \mathbf{p}'_i \cdot \mathbf{p}'_i + U_c(\mathbf{q}) \tag{3.2}$$

where $n_c$ is the number of atoms in the cell-ensemble $c$, $U_c(\mathbf{q})$ is the atomistic potential, $\bar{\mathbf{p}}_i$ and $\mathbf{p}'_i$ are, respectively, the coarse scale and fine scale linear momentum vectors of the $i$-th atom. Here and in the following the subscript $i$ is used to denote the quantities of the $i$-th atom. Note that each cell-ensemble has only one node, so the numberings $I$ and $c$ have one-to-one correspondence (see Fig. 2).

The two-scale equations of motion are then derived from Eq. (3.2) as

$$\dot{\mathbf{q}}_i = \frac{\partial H_c^{\text{adia}}}{\partial \mathbf{p}_i} = \frac{\bar{\mathbf{p}}_i}{m_i} + \frac{\mathbf{p}'_i}{m_i} \quad \text{and} \quad \dot{\mathbf{p}}_i = -\frac{\partial H_c^{\text{adia}}}{\partial \mathbf{q}_i} = -\frac{\partial U(\mathbf{q})}{\partial \mathbf{q}_i} = \mathbf{F}_i, \tag{3.3}$$

$$\dot{\bar{\mathbf{q}}}_i = \frac{\partial H_c^{\text{adia}}}{\partial \bar{\mathbf{p}}_i} = \frac{\bar{\mathbf{p}}_i}{m_i} \quad \text{and} \quad \dot{\bar{\mathbf{p}}}_i = -\frac{\partial H_c^{\text{adia}}}{\partial \bar{\mathbf{q}}_i} = \mathbf{F}_j \cdot \frac{\partial \mathbf{q}_j}{\partial \bar{\mathbf{q}}_i}, \tag{3.4}$$

where $\mathbf{F}_i$ denotes the external force acting on the atom $i$. From Eq. (3.3), the fine scale equations of motion may be expressed in terms of $\mathbf{q}_i$ and $\mathbf{p}'_i$ as follows,

$$\dot{\mathbf{q}}_i = \frac{\bar{\mathbf{p}}_i}{m_i} + \frac{\mathbf{p}'_i}{m_i} \quad \text{and} \quad \dot{\mathbf{p}}'_i = \mathbf{F}_i - \dot{\bar{\mathbf{p}}}_i. \tag{3.5}$$

To couple the fine scale motions of atoms with the coarse scale heat conduction, we introduce a local Nośe–Hoover thermostat in each cell-ensemble such that the fine scale equations of motion in Eq. (3.5) become

$$\dot{\mathbf{q}}_i = \frac{\bar{\mathbf{p}}_i}{m_i} + \frac{\mathbf{p}'_i}{m_i} \quad \text{and} \quad \dot{\mathbf{p}}'_i = \mathbf{F}_i - \dot{\bar{\mathbf{p}}}_i - \xi_c \mathbf{p}'_i \tag{3.6}$$

$\forall i \in \mathbf{n}_c, \quad \mathbf{n}_c = \{1, \ldots, n_c\}$ and

$$\dot{\xi}_c = \frac{1}{\Theta_c} \left( \sum_{i \in \mathbf{n}_c} \frac{\mathbf{p}'_i \cdot \mathbf{p}'_i}{m_i} - 3n_c k_B T_c \right), \tag{3.7}$$

where $k_B$ is the Boltzmann constant, $\xi_c$ is an auxiliary variable [Hoover, 1985; Nośe, 1984, 1986], $\mathbf{\Theta}_c$ is the pseudo mass of $\xi_c$, and the local thermodynamic temperature $T_c$ for cell-ensemble $c$ is the coarse scale temperature at the governing FE node $I$.

As introduced in Sec. 2, a distributed Nośe–Hoover thermostat network is used in the MS-NEMD simulation to ensure each cell-ensemble reaching to a local equilibrium state within one coarse scale time step. Moreover, based on the inhomogeneous coarse scale temperature, the distributed Nośe–Hoover thermostat network provides a source of random forces to drive the fine scale system out of equilibrium.

The conventional Nośe–Hoover thermostat renders the MD system a canonical ensemble. The authors have proved in a recent paper [Li *et al.*, 2008] that the proposed distributed Nośe–Hoover thermostat network provides a similar role in the nonequilibrium simulation, and it yields a local canonical distribution function for nonequilibrium thermodynamics. This is superior to the algorithm proposed by Liu and Li [2007]. Using the canonical approach and the local equilibrium approach to study nonequilibrium systems is not new, and it can be traced back to Kawasaki and Gunton [1973] and Mori [1958] and more recently Edwards *et al.* [2005] and Taniguchi and Morriss [2004]. The contribution of this work is to rigorously apply the local canonical distribution approach to MD in a multi-scale setting.

## 4. The Coarse Scale Model

In discrete-to-continuum multi-scale computations, we want our coarse scale model to be a coarse-grained one, in the sense that it needs to be consistent with the fine scale model. This means we have to incorporate atomic information into the coarse scale level. Traditional FE methods do not satisfy this criterion, since they use empirical constitutive models. In the proposed MS-NEMD model, the coarse scale mean field is concurrently solved by the FE method based on a coarse-grained thermodynamics model [Jiang *et al.*, 2005; Weiner, 1983]. The formulation is based on a coarse-grained Helmholtz free energy. It stems from the principles described by Weiner [1983] and is derived with the assumptions of harmonic approximation and the Cauchy–Born rule. In this paper, we will use the coarse-grained Helmholtz free energy to derive macroscopic quantities in coupled thermomechanical equations.

The main provision of the classical Cauchy–Born rule is that within a local region, the deformation gradient is assumed to be a constant and the underlying atomic lattice will deform the same way. In Liu and Li [2007], a local region is viewed as an FE and the coarse-grained thermodynamics model is formulated within each FE. In this paper, we formulate the coarse-grained model within each cell-ensemble instead of within each element, because one of the basic assumptions

of the proposed MS-NEMD model is that within the time scale of the coarse grain each cell-ensemble can reach to a local equilibrium state, which means that the temperature is a constant in a cell-ensemble rather than in an element, see Fig. 2.

To use the Cauchy–Born rule in the multi-scale analysis, we have constructed a coarse scale Cauchy–Born rule as

$$\bar{\mathbf{r}}_{i\alpha} = \bar{\mathbf{F}}^c \cdot \mathbf{R}_{i\alpha}, \tag{4.1}$$

where $\bar{\mathbf{r}}_{i\alpha}$ denotes the coarse scale projection of the position vector between atoms $i$ and $\alpha$ in the deformed lattice, $\mathbf{R}_{i\alpha}$ denotes the original bond vector in referential space, and $\bar{\mathbf{F}}^c$ denotes the average deformation gradient within a cell-ensemble $c$, which is approximated as the value of the coarse scale deformation gradient evaluated at the nodal point $I$ since the cell-ensemble $c$ contains only one nodal point $I$ ($I$ and $c$ have the one-to-one correspondence).

If we only consider the pair potential, the total potential energy in a Voronoi cell-ensemble $c$ can be written as

$$U_0 = \frac{1}{2}\sum_{i=1}^{n_c}\sum_{\alpha=1}^{n_b}\varphi(r_{i\alpha}), \tag{4.2}$$

where $n_c$ is the total number of atoms in the cell-ensemble $c$, $n_b$ is the total number of pair atomistic bonds in a unit cell, e.g. $n_b = 4$ for a cubic lattice, and $r_{i\alpha} = |\mathbf{r}_{i\alpha}|$ is the length of the position vector. For the multi-scale Cauchy–Born rule, we assume that $U_0$ is approximated as the function of the mean value of the deformation gradient within the cell-ensemble, i.e.

$$U_0(r_{i\alpha}) \approx U_0(\bar{r}_{i\alpha}) = U_0(\bar{\mathbf{F}}^c), \tag{4.3}$$

where $\bar{r}_{i\alpha} = |\bar{\mathbf{r}}_{i\alpha}|$, which is related to $\bar{\mathbf{F}}^c$ by Eq. (4.1).

Based on the harmonic approximation and the Cauchy–Born rule, the coarse-grained Helmholtz free energy in a cell-ensemble $c$ may be written as [Weiner, 1983]

$$\Phi^c(\bar{\mathbf{F}}^c, T_c) = U_0(\bar{\mathbf{F}}^c) + k_B T_c \sum_{i=1}^{n_c}\sum_{k=1}^{3}\log\left[2\sinh\left(\frac{\hbar\omega_{ik}(\bar{\mathbf{F}}^c)}{4\pi k_B T_c}\right)\right], \tag{4.4}$$

where $\hbar$ is Planck's constant divided by $2\pi$; $T_c$ is the coarse scale thermodynamic temperature for the cell-ensemble $c$; and $\omega_{ik}$ are three normal mode frequencies for the atom $i$, which depend on $\bar{\mathbf{F}}^c$ through $\bar{\mathbf{r}}_{i\alpha}$ and can be determined via harmonic approximation [Jiang *et al.*, 2005].

Note that in the proposed MS-NEMD model, $T_c$ is updated based on fine scale atomistic velocities:

$$T_c = \frac{2}{3(n_c - 1)k_B}\left\langle\sum_{i=1}^{n_c}\frac{\mathbf{p}_i' \cdot \mathbf{p}_i'}{2m_i}\right\rangle, \tag{4.5}$$

where $\langle\cdot\rangle$ denotes averaging in time.

With $\Phi^c$ available, we can derive the expressions for the state variables such as the first Piola–Kirchhoff stress $\mathbf{P}^c$, the specific heat at constant volume $C_V^c$ and the

specific heat at constant temperature $\mathbf{C}_T^c$:

$$\begin{aligned}\mathbf{P}^c(\bar{\mathbf{F}}^c, T_c) &= \frac{1}{\Omega_c}\frac{\partial \mathbf{\Phi}^c}{\partial \bar{\mathbf{F}}^c} \\ &= \frac{1}{\Omega_c}\left\{\frac{1}{2}\sum_{i=1}^{n_c}\sum_{\alpha=1}^{n_b}\varphi'(\bar{r}_{i\alpha})\frac{\bar{\mathbf{r}}_{i\alpha}\otimes\mathbf{R}_{i\alpha}}{\bar{r}_{i\alpha}}\right. \\ &\quad \left. + \frac{\hbar}{4\pi}\sum_{i=1}^{n_c}\sum_{k=1}^{3}\coth\left(\frac{\hbar\omega_{ik}(\bar{\mathbf{F}}^c)}{4\pi k_B T_c}\right)\left[\sum_{\alpha=1}^{n_b}\omega'_{ik}(\bar{r}_{i\alpha})\frac{\bar{\mathbf{r}}_{i\alpha}\otimes\mathbf{R}_{i\alpha}}{\bar{r}_{i\alpha}}\right]\right\}, \qquad (4.6)\end{aligned}$$

$$C_V^c(\bar{\mathbf{F}}^c, T_c) = -T_c\frac{\partial^2\mathbf{\Phi}^c}{\partial T_c^2} = \frac{\hbar^2}{16\pi^2 k_B T_c^2}\sum_{i=1}^{n_c}\sum_{k=1}^{3}\frac{\left(\omega_{ik}(\bar{\mathbf{F}}^c)\right)^2}{\sinh^2\left(\frac{\hbar\omega_{ik}(\bar{\mathbf{F}}^c)}{4\pi k_B T_c}\right)}, \qquad (4.7)$$

$$\begin{aligned}\mathbf{C}_T^c(\bar{\mathbf{F}}^c, T_c) &= -T_c\frac{\partial^2\Phi^c}{\partial T_c\partial\bar{\mathbf{F}}^c} \\ &= \frac{-\hbar^2}{16\pi^2 k_B T_c}\sum_{i=1}^{n_c}\sum_{k=1}^{3}\frac{\omega_{ik}(\bar{\mathbf{F}}^c)}{\sinh^2\left(\frac{\hbar\omega_{ik}(\bar{\mathbf{F}}^c)}{4\pi k_B T_c}\right)}\left[\sum_{\alpha=1}^{n_b}\omega'_{ik}(\bar{r}_{i\alpha})\frac{\bar{\mathbf{r}}_{i\alpha}\otimes\mathbf{R}_{i\alpha}}{\bar{r}_{i\alpha}}\right] \qquad (4.8)\end{aligned}$$

in which $\Omega_c$ denotes the volume of the cell-ensemble $c$. Note that in the proposed MS-NEMD algorithm, the above transport coefficients will be later updated based on the fine scale computation via the response theory.

Our coarse-grained model is built in conjunction with the FE method. To establish the FE formulation, we start with the governing equations at the coarse scale level. They include: (i) the equation of motion, and (ii) the first law of thermodynamics. The equation of motion at coarse scale can be written as

$$\nabla_{\mathbf{X}}\cdot\mathbf{P} + \rho_0\mathbf{B} = \rho_0\ddot{\bar{\mathbf{u}}}, \quad \forall\mathbf{X}\in\Omega_0, \qquad (4.9)$$

where $\Omega_0$ denotes the entire domain of the problem, $\mathbf{X}$ denotes the spatial position vector, $\bar{\mathbf{u}}(\mathbf{X})$ is the continuous displacement field, $\rho_0$ is the density in material configuration, $\mathbf{B}$ is the body force, $\nabla_{\mathbf{X}}$ is the material divergence operator, and $\mathbf{P}$ is defined by

$$\mathbf{P}(\mathbf{X}) := \sum_{c=1}^{n_{\text{cell}}}\mathbf{P}^c\chi(\Omega_c). \qquad (4.10)$$

Note that $n_{\text{cell}} = n_{\text{node}}$ denotes the number of cell-ensembles/FE nodes, and $\chi(\Omega_c)$ is the characteristic function of each cell-ensemble,

$$\chi(\Omega_c) := \begin{cases}1, & \forall\mathbf{X}\in\Omega_c \\ 0, & \forall\mathbf{X}\notin\Omega_c\end{cases}. \qquad (4.11)$$

Consider the first law of thermodynamics:

$$\dot{w} = \rho_0 z - \nabla_{\mathbf{X}}\cdot\mathbf{Q} + \mathbf{P}:\dot{\bar{\mathbf{F}}}, \qquad (4.12)$$

where $w$ is the internal energy per unit reference volume, $z$ is the heat source per unit mass, $\mathbf{Q}$ is the Piola–Kirchhoff heat flux, and $\bar{\mathbf{F}} = \mathbf{I} + \frac{\partial \bar{\mathbf{u}}}{\partial \mathbf{X}}$. For the heat flux $\mathbf{Q}$, we exploit Fourier's law in the material configuration

$$\mathbf{Q} = -\mathbf{K} \cdot \nabla_{\mathbf{X}} T, \tag{4.13}$$

where $\mathbf{K}$ is the thermal conductivity. Then the first law provides the following heat conduction equation

$$\frac{\mathbf{C}_T}{\Omega_0} : \dot{\bar{\mathbf{F}}} + \frac{C_V}{\Omega_0} \dot{T} = \rho_0 z + \nabla_{\mathbf{X}} \cdot \mathbf{K} \cdot \nabla_{\mathbf{X}} T, \tag{4.14}$$

where $C_V$ and $\mathbf{C}_T$ are defined by

$$C_V(\mathbf{X}) := \sum_{c=1}^{n_{\text{cell}}} \frac{\Omega_0}{\Omega_c} C_V^c \chi(\Omega_c), \tag{4.15}$$

$$\mathbf{C}_T(\mathbf{X}) := \sum_{c=1}^{n_{\text{cell}}} \frac{\Omega_0}{\Omega_c} \mathbf{C}_T^c \chi(\Omega_c). \tag{4.16}$$

Equations (4.9) and (4.14) form the complete set of governing equations for the coarse-grained model. In computations, we use the coarse scale velocity and acceleration to update the atomistic velocity and acceleration. The coarse scale thermodynamic temperature is used to set up heat reservoirs for the fine scale computations. On the other hand, the fine scale atomistic position can be used to calculate the atomistic force which is then mapped to FE nodes to obtain the internal force for the coarse scale computations. The fine scale atomistic velocity can be used to update coarse scale temperature. By doing so, the coarse scale model is coupled with the fine scale model.

## 5. Numerical Examples

Two numerical examples are presented in this paper to illustrate the effectiveness of the proposed MS-NEMD model.

### 5.1. *A one-dimensional shock wave propagation*

The first example is the simulation of a shock wave propagation along one-dimensional (1D) lattice. A special type of Frenkel–Kontorova potential, or the FPU-$\beta$ potential [Lepri *et al.*, 2003], is used,

$$U(\mathbf{q}) = \sum_i \left( \frac{k}{2} \left( |q_i - q_j| - a \right)^2 + \frac{\mu}{2} \left( q_i - a \operatorname{int}(q_i/a) \right)^2 \right.$$
$$\left. - \frac{\mu}{24} (q_i - a \operatorname{int}(q_i/a))^4 \right), \quad |i - j| = 1.$$

The following normalised parameters are used: $a = 1, k = 1, \mu = 0.7, m_i = 1, \tilde{k}_B = k_B t_c^2 / m_c L_c^2$ and $\tilde{\hbar} = \hbar t_c / m_c L_c^2$, where $m_c, L_c$ and $t_c$ are characteristic mass, length

and time, respectively. They are chosen as: $m_c = 26.98\,\text{amu}$, $L_c = 3.253\,\text{Å}$ and $t_c = 2.0 \times 10^{-13}\,\text{s}$, respectively. A domain of [0, 1000] with 1001 atoms is considered. There are 50 FEs and each of them consists of 20 atoms. The normalised coarse scale time step is 0.1 and the normalised fine scale time step is 0.01.

In the simulation, a constant external force $f = 0.03$, which is slightly lower than the critical force (the Peierls force), is applied to every atom along the 1D lattice. A strong discontinuity in displacement field (dislocation) is prescribed in the middle of the lattice. Figs. 4(a)–4(c) show the time histories of the displacement profiles with initial temperatures $T_0 = 0, 100$ and 200 K, respectively. It can be observed that the shock does not propagate along the lattice when $T_0 = 0$ and 100 K. Whereas when $T_0 = 200\,\text{K}$, the shock wave starts moving from right to left, which indicates the thermal activation of shock wave or dislocation motions. Figs. 4(d)–4(f) display the time histories of the fine scale temperature profiles when $T_0 = 0, 100$ and 200 K, respectively. One can observe that when the initial temperature increases, the fine scale temperature distribution is visibly larger. It indicates that the thermal–mechanical interaction is more significant in the case of $T_0 = 200\,\text{K}$ and hence, the thermal activation of shock wave occurs when the initial temperature is increased to 200 K. To the authors' best knowledge, this is the first successful numerical simulation of thermal activation of "dislocation" under nonequilibrium conditions. The fine scale calculation provides the essential source for thermal–mechanical coupling at both scales, and the activation of dislocation is clearly due to thermal fluctuations.

We have also performed the direct NEMD simulation with a fixed temperature of 200 K at the boundary ends. The results are compared with that of the present MS-NEMD simulation with the initial temperature of 200 K. It is found that the direct NEMD simulation fails to predict thermal-activation of shock wave or dislocation, whereas the MS-NEMD simulation can do so, see Figs. 5(a) and 5(b). By comparing the instantaneous temperature profiles obtained by the two simulations in Figs. 5(c) and 5(d), it is observed that the instantaneous temperature distribution obtained by the MS-NEMD simulation exhibits larger fluctuations than that of the direct NEMD simulation. The thermal–mechanical interaction is constrained in the direct NEMD simulation, which may be due to the use of the micro-canonical MD simulation in the interior of the simulation domain. While the inherent statistical or thermodynamic structures in the MS-NEMD simulation enable it to produce thermal fluctuations that are responsible for exciting unstable dislocation motions. This example clearly indicates an advantage of the proposed MS-NEMD simulation over the direct NEMD simulation.

### 5.2. *A two-dimensional shock wave propagation*

In the second example, we simulate a shock wave propagation in a cubic lattice. The dimension of the computation domain is $[-100h_a, 100h_a] \times [-100h_a, 100h_a]$, where $h_a = 3.253\,\text{Å}$ is the interatomic spacing. By choosing characteristic length

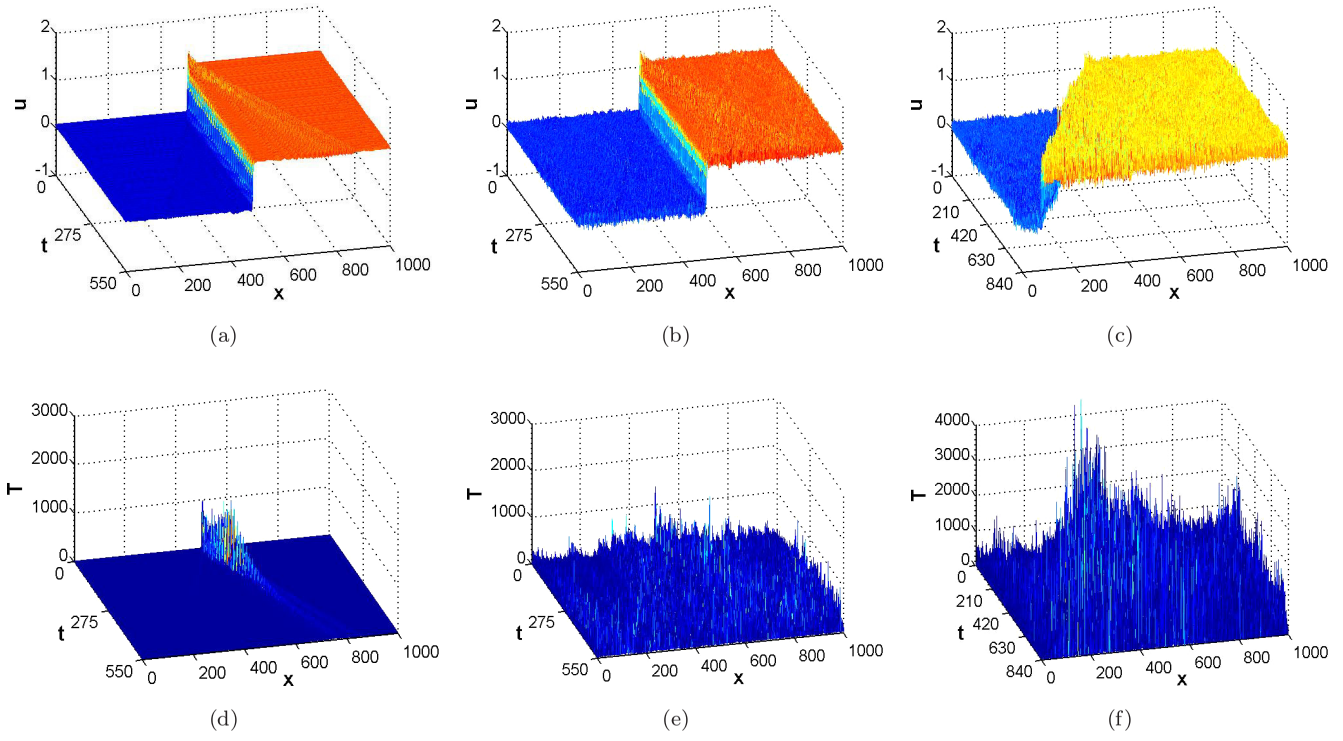


Fig. 4. Displacement profiles with initial temperatures at (a) $T_0 = 0\,\mathrm{K}$, (b) $T_0 = 100\,\mathrm{K}$ and (c) $T_0 = 200\,\mathrm{K}$; instantaneous temperature profiles with initial temperatures at (d) $T_0 = 0\,\mathrm{K}$, (e) $T_0 = 100\,\mathrm{K}$ and (f) $T_0 = 200\,\mathrm{K}$.

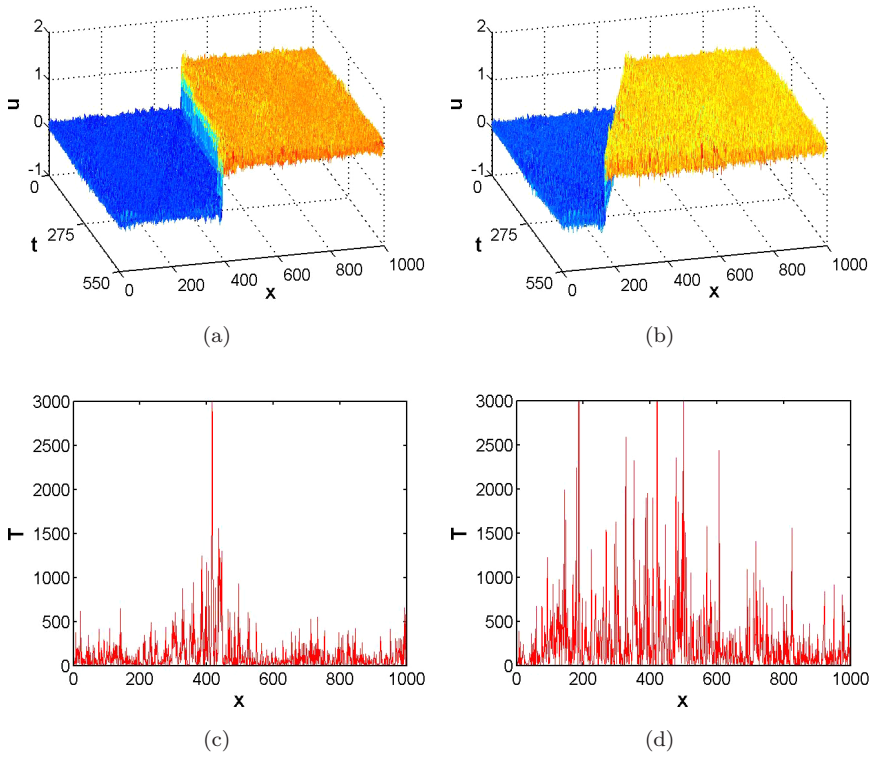


Fig. 5. Displacement profiles obtained by (a) direct NEMD simulation and (b) MS-NEMD simulation; instantaneous temperature profiles obtained by (c) direct NEMD simulation and (d) MS-NEMD simulation.

as $L_c = h_a$, the normalised interatomic spacing is 1 and the normalised dimension of the domain is $[-100, 100] \times [-100, 100]$. We simulate the problem with 40401 atoms and 800 linear triangle elements. There are total of 441 FE nodes and each of them represents a Voronoi cell-ensemble of 100 atoms. An initial out-of-plane displacement or dislocation is prescribed as: $q(r) = 1$ for $r \leq 20$. A constant out-of-plane force $f = 0.04$, which is slightly higher than the critical force, is applied to every atom. The FPU-$\beta$ potential is used as the atomistic potential,

$$U(\mathbf{q}) = \sum_{i,j} \left( \frac{k}{2}(q_{i,j} - q_{m,n})^2 + \frac{\mu}{2}(q_{i,j} - \text{int}(q_{i,j}))^2 - \frac{\mu}{24}(q_{i,j} - \text{int}(q_{i,j}))^4 \right),$$

in which $|(i + j) - (m + n)| = 1$, or $|i - m| = 1, |j - n| = 1$, the subscript indices, $i$ and $j$, denote the position of a discrete point in the 2D plane. The parameters used in computations are the same as those in the example of 1D shock wave propagation. The normalised coarse scale time step is 0.2, and the normalised fine scale time step is 0.02. The initial temperature is chosen as $T_0 = 100\,\text{K}$ that distributes uniformly throughout the domain.

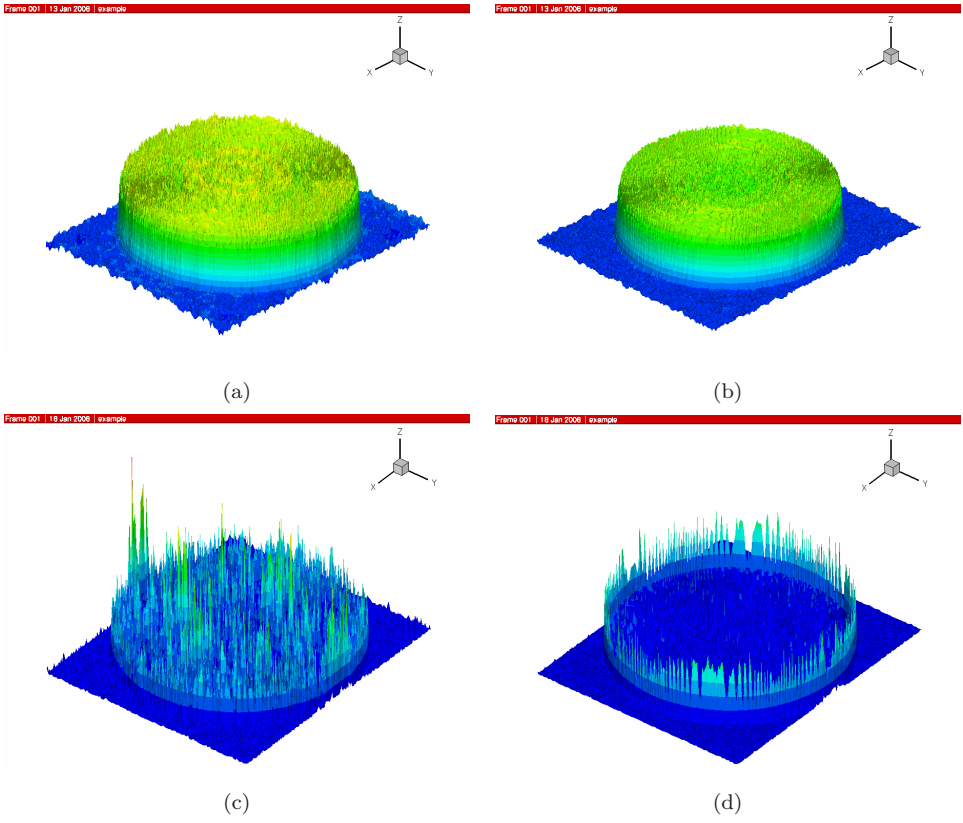


Fig. 6. A 2D shock wave propagation: displacement profiles obtained by (a) MS-NEMD simulation and (b) direct NEMD simulation; instantaneous temperature profiles obtained by (c) MS-NEMD simulation and (d) direct NEMD simulation.

In Figs. 6(a) and 6(b), one may find that the results obtained by the MS-NEMD simulation show visibly larger displacement fluctuations than that of the direct NEMD simulation. The instantaneous temperature profile as shown in Fig. 6(c) obtained by the MS-NEMD simulation indicates that the temperature amplitude in the region that shock wave passes through will not drop down to the initial temperature, and it will remain fluctuating for some time. Whereas based on the temperature profile as shown in Fig. 6(d) obtained by the direct NEMD simulation, the temperature inside the zone that shock wave passes through will immediately drop to the initial temperature. This cannot be true because the time scale for heat diffusion is much larger than the simulation time reported.

## 6. Conclusions

An MS-NEMD algorithm has been developed based on the postulate of local equilibrium and the fluctuation dissipation theorem. This is accomplished by setting

the Nośe–Hoover thermostat in each cell-ensemble to form a distributed thermostat network, which may yield a local canonical distribution function for NEMD. The underline principle for the distributed Nośe–Hoover thermostat approach is to use local thermodynamic equilibrium assumption to study general nonequilibrium processes. Moreover, the distributed Nośe–Hoover thermostat network provides a source of random forces based on mean field intensity to drive the fine scale system out of equilibrium.

A detailed description and discussion on both the theory and algorithm of the MS-NEMD simulation, including verification and validation, size effects of continuum FE or coarse grain and the calculation of transport coefficients based on the fine scale computations, will be presented in coming papers.



## Acknowledgements

This work is supported by a grant from NSF (Grant no. CMS-0239130), which is greatly appreciated. The authors would like to thank for Dr. Xiaohu Liu for his early participation in this work.

## References

Baranyai, A. [1996] *Phys. Rev. E* **54**, 6911.
Bright, J. N. and Evans, D. J. [2005] *J. Chem. Phys.* **122**, 194106.
Chen, G. [2005] *Nanoscale Energy Transport and Conversion* (Oxford University Press, Oxford).
Edwards, B. and Dressler, M. J. [2001] *Non-Newtonian Fluid Mech.* **96**, 163.
Edwards, B., Baig, C. and Keffer, D. J. [2005] *J. Chem. Phys.* **123**, 1141106.
Evans, D. J. and Morriss, G. P. [1990] *Statistical Mechanics of Nonequilibrium Liquids* (Academic Press, Inc., San Diego).
Evans, D. J. and Morriss, G. P. [1984] *Phys. Rev. A* **30**, 1528.
Evans, D. J., Hoover, W. G., Failor, B. H., Moran, B. and Ladd, A. J. C. [1983] *Phys. Rev. A* **8**, 1016.
Galea, T. M. and Attard, P. [2002] *Phys. Rev. E* **66**, 041207.
Hoover, W. G. [1980] in *Systems Far From Equilibrium*, ed. L. Garrido (Springer-Verlag).
Hoover, W. G. [1983] *Ann. Rev. Phys. Chem.* **34**, 103.
Hoover, W. G. [1985] *Phys. Rev. A* **31**, 1695.
Jiang, H., Huang, Y. and Hwang, K. C. [2005] *ASME J. Eng. Mater. Technol.* **127**, 408.
Kawasaki, K. and Gunton, D. [1973] *Phys. Rev. A* **8**, 2048.
Knap, J. and Ortiz, M. [2001] *J. Phys. Mech. Solids* **49**, 1899.
Lepri, S., Livi, R. and Politi, A. [2003] *Phys. Rep.* **377**, 1.
Li, S., Liu, X., Agrawal, A. and To, A. [2006] *Phys. Rev. B* **74**, 045418.
Li, S., Sheng, N. and Liu, X. [2008] *Chem. Phys. Lett.* **451**, 293.
Liu, X. and Li, S. [2007] *J. Chem. Phys.* **126**, 124105.
Müller-Plathe, F. [1997] *J. Chem. Phys.* **106**, 6082.
Mori, H. [1958] *Phys. Rev.* **112**, 1829.
Nośe, S. [1984] *Mol. Phys.* **52**, 255.
Nośe, S. [1986] *Mol. Phys.* **57**, 187.
Qiang, D., Faber, V. and Gunzburger, M. [1999] *SIAM Rev.* **41**, 637.

Rudd, R. E. and Broughton, J. Q. [1998] *Phys. Rev. B* **58**, R5893.
Rudd, R. E. and Broughton, J. Q. [2005] *Phys. Rev. B* **72**, 144104.
Tadmor, E., Ortiz, M. and Phillips, R. [1996] *Phil. Mag. A* **73**, 1529.
Tang, Z., Zhao, H., Li, G. and Aluru, N. [2006] *Phys. Rev. B* **74**, 064110.
Taniguchi, T. and Morriss, G. [2004] *Phys. Rev. E* **70**, 056124.
To, A. and Li, S. [2005] *Phys. Rev. B* **72**, 035414.
Tuckerman, M. E., Mundy, C. J., Balasubramanian, S. and Klein, M. L. [1997] *J. Chem. Phys.* **106**, 5616.
Wagner, G. J. and Liu, W. K. [2003] *J. Comput. Phys.* **190**, 249.
Wagner, G. J., Karpov, E. G. and Liu, W. K. [2004] *Comput. Meth. Appl. Mech. Eng.* **193**, 1579.
Weiner, J. H. [1983] *Statistical Mechanics of Elasticity* (John Wiley & Sons, New York).
Zhang, F., Isbister, D. J. and Evans, D. J. [2000] *Phys. Rev. E* **61**, 3541.